KSME

Springer

Journal of Mechanical Science and Technology 37 (5) 2023

Original Article
DOI 10.1007/s12206-023-0436-3

Keywords:
· Heat exchanger
· Offset-strip fin
· Artificial neural network
· Thermo-hydraulic performance

Correspondence to:
Man Yeong Ha
myha@pusan.ac.kr

Citation:
Kim, S., Seo, Y. M., Yoon, S. Y., Kim, S., Pandey, S., Ha, M. Y. (2023). Thermo-hydraulic performance prediction for offset-strip fin heat exchangers using artificial neural networks. Journal of Mechanical Science and Technology 37 (5) (2023) 2623~2638.
http://doi.org/10.1007/s12206-023-0436-3

Received July 27th, 2022
Revised December 12th, 2022
Accepted January 17th, 2023

† Recommended by Editor Tong Seop Kim

Thermo-hydraulic performance prediction for offset-strip fin heat exchangers using artificial neural networks

Sangmin Kim[1], Young Min Seo[2], Sang Youl Yoon[3], Seokho Kim[4], Sudhanshu Pandey[3] and Man Yeong Ha[1]

[1]School of Mechanical Engineering, Pusan National University, Busan, Korea, [2]Korea Electrotechnology Research Institute, Changwon, Korea, [3]Rolls-Royce and Pusan National University Technology Centre, Busan, Korea, [4]Department of Mechanical Engineering, Changwon National University, Changwon 641-773, Korea

Abstract In this study, an artificial neural network (ANN) model was applied to predict the thermo-hydraulic performance of the offset-strip fin heat exchanger. The ANN model was used for predicting the thermo-hydraulic performance to improve the prediction accuracy and extend the applicable range compared to the results of using the empirical equations reported in previous studies. The main parameters of these empirical equations were fin height ($0.134 < \alpha < 0.997$), fin length ($0.012 < \delta < 0.048$), fin width ($0.041 < \gamma < 0.121$), and Reynolds number ($120 < Re < 10^4$). In addition, the Fanning friction factor f and the Colburn factor j were considered as the outputs of the ANN model. The impact of the parameters on the thermo-hydraulic performance of the heat exchanger was quantitatively evaluated, and the prediction accuracy was improved over a wide range for the thermo-hydraulic performance generated by the ANN model. Thus, the results obtained using the ANN model agreed well with the experimental data over a wider range than possible for the previous empirical correlations, showing extremely high accuracy and validity of the ANN model in comparison to the empirical equations.

1. Introduction

The offset-strip fin heat exchanger is a type of plate fin heat exchangers (PFHEs) with a rectangular cross section cut into small strips of fin length and displaced by the fin pitch in the transverse direction. This offset-strip fin has relatively better thermo-hydraulic performance than a plain-plate fin heat exchanger, which is a simple type of PFHEs. The improved heat transfer is attributed to the periodic growth in the thermal and hydraulic boundary layers on the offset-strip fin. However, an increase in heat transfer is always accompanied by an increase in pressure drop caused by increased frictional loss and form drag on the offset-strip fin. The offset-strip fin heat exchanger has been widely applied across industries such as recuperators [1] and evaporators and condensers in air conditioners [2] because of its high thermo-hydraulic performances and compact size.

Accurate prediction of the thermo-hydraulic performance of the offset-strip fin heat exchangers is important in the design process of the heat exchanger. However, to develop a calculation model that can accurately predict the thermo-hydraulic performance of this type of heat exchanger, a large number of geometrical parameters involved in the prediction model should be considered. Some representative geometrical parameters such as the fin length l, fin height h, thickness t, and fin width w are shown in Fig. 1. Several experimental and numerical studies [3-10] investigated the thermo-hydraulic performances of this type of heat exchangers. In these studies, prediction models were developed to calculate the thermo-hydraulic performances of the heat exchangers using experimental and numerical results for different geometrical parameters, and attempts were made to improve the prediction accuracy.

Kays and London [3] numerically investigated the thermo-hydraulic performances of various

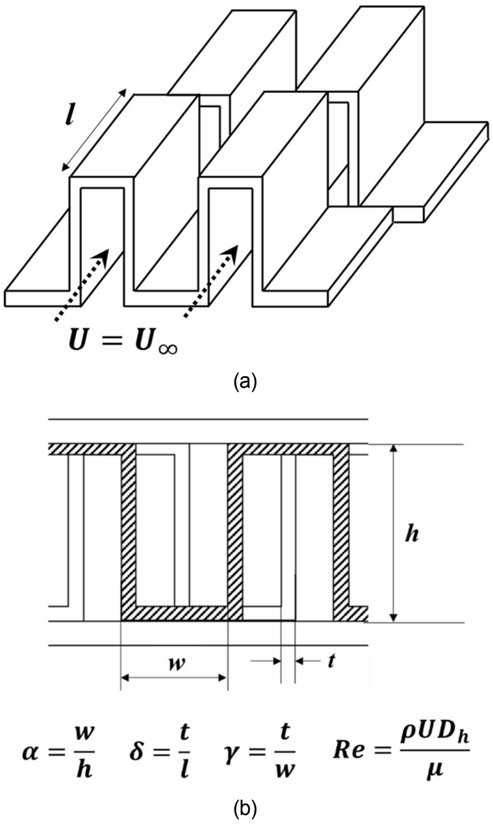

Fig. 1. Physical model of the offset-strip fins and their geometric parameters: (a) isometric view; (b) frontal cross-sectional view.

fin-type heat exchangers and provided the modified laminar boundary layer solution for each type and experimental data for thermo-hydraulic performances of these heat exchangers. Manson [4] proposed predictive equations for the thermo-hydraulic performances of offset-strip fin heat exchangers and suggested dimensionless design parameters for the empirical model of these heat exchangers. Over a wide range of design parameters, the heat transfer characteristics agreed well with the experimental data. The empirical models for frictional loss in these heat exchangers showed relatively lower accuracies in the transition range (Laminar to Turbulent) at Re = 3500 than in the other prediction ranges. Wieting [5] implemented power law curve fittings using data for 22 geometries for both laminar and turbulent flows separately. For the transition region, an extrapolation method was used to predict the Fanning friction factor f and Colburn factor j. Dimensionless parameters for the offset-strip fin were suggested. Compared to the models developed for other types of PFHEs, the accuracy of the empirical models for predicting the thermo-hydraulic performance of the offset-strip fin heat exchangers should be improved.

Recently, artificial neural network (ANN) algorithms have been applied to improve the accuracies of empirical models. ANN models have been developed for various engineering applications such as heating, ventilation, and air-conditioning, and for equipment such as the gas turbine [11-14] and improvements were achieved in the model prediction accuracies for the thermo-hydraulic performances of each system. To improve the empirical models for thermo-hydraulic performances in a heat exchanger, ANN models were applied in recent studies, and significant improvements in accuracies were realized [15-18].

Arturo et al. [15] investigated heat-rate estimation of heat exchangers used in refrigeration applications based on the ANN. The capability of the ANN model was demonstrated using a limited experimental dataset for modeling the heat transfer characteristics in refrigerator systems. Gerardo et al. [16] reported that ANN algorithms with a sigmoid activation function can be applied for nonlinear problems such as convection problems, which are otherwise hard to identify with physical variables. Additionally, they applied the ANN models to predict the thermo-hydraulic performances of single-row, fin-tube type heat exchangers and obtained higher accuracies with smaller scattering compared to the power-law correlation approach. Esfe [17] developed a prediction model for thermo-hydraulic performances in heat exchangers and built an ANN model with the experimental datasets, including the heat transfer and flow characteristics in a nanofluid-based double-tube heat exchanger. The ANN model gave higher regression coefficients compared to the previously reported prediction models. Patra et al. [18] applied ANN models to model intermediate heat exchangers in nuclear reactors. The ANN models were trained based on the theoretical calculation results, which were obtained for the primary and secondary outlet temperatures of an intermediate heat exchanger.

From the literature review of ANN modeling for predicting heat exchanger performance, it is seen that the ANN can be a useful method to predict the thermo-hydraulic performances in offset-strip fin heat exchangers because of its higher accuracy compared to other approaches. However, few studies explored the use of ANN models for predicting the thermo-hydraulic performances of heat exchangers.

The ANN model has an advantage over empirical models as the ANN model has higher accuracy in predicting the thermo-hydraulic performances. According to recent studies, the ANN is a powerful algorithm to improve the accuracies of empirical models for the thermo-hydraulic performances of offset-strip fin heat exchangers, which exhibit non-linear relationships with multiple inputs and outputs.

All of these studies revealed that the empirical models have their own limitations in terms of accuracies in the range of Re < 500 and Re > 8000 to predict the thermo-hydraulic performances of offset-strip fin heat exchangers. Additionally, thermo-hydraulic performance is hard to predict owing to its nonlinear relationships with multiple inputs and outputs. Hence, this study suggests an alternative ANN-based approach to predict the thermo-hydraulic performances of the offset-strip fin heat exchanger. The objective was to improve the prediction accuracy and extend the applicable range compared to the results of previous empirical models. In addition, the relative impacts of each input parameter were evaluated to explain how the input parameters influence the thermo-hydraulic performance.

2. Numerical methodology

2.1 Datasets on thermo-hydraulic performance for heat exchangers

Many researchers [3-10] reported experimental findings on the thermo-hydraulic performances of heat exchangers with various offset-strip fin geometries. Overall, 160 experimental datasets [3-10] were selected and trained using the present ANN model. The experimental datasets were divided into two datasets according to the design parameter range considered by Manglik and Bergles [9]. The first dataset contained 41 experimental data that were covered by Manglik and Bergles's model [9]. The second dataset contained the remaining 119 experimental data that could not be covered by their model [9].

2.2 Previous model on thermo-hydraulic performance for heat exchanger

The thermo-hydraulic performances of heat exchangers can be characterized by non-dimensional parameters such as f and j, which are defined as shown in Eqs. (1) and (2):

$$f = \frac{\tau}{\rho \frac{u^2}{2}} \tag{1}$$

$$j = StPr^{\frac{2}{3}}. \tag{2}$$

Here, the Stanton number (St) and Prandtl number (Pr) are defined as follows:

$$Pr = \frac{\mu c_p}{\lambda} \tag{3}$$

$$St = \frac{q_w}{c_p G(T_m - T_w)} = \frac{h}{Gc_p} \tag{4}$$

where ρ, μ, c_p, λ, and h are density, dynamic viscosity, specific heat, thermal conductivity, and convective heat transfer coefficient, respectively. The wall shear stress τ and wall heat flux q_w are defined at mass flux G. In this study, the working fluid for the dataset is all air, the value of Pr can be assumed as 0.7.

An analysis of the thermo-hydraulic performance reported in existing studies [3-9] was performed to determine design parameters of offset-strip fin heat exchanger. Table 1 summarizes the existing empirical models for predicting the thermo-hydraulic performances of offset-strip fin heat exchanger and lists the data sources, types of databases, and application ranges.

In an earlier study, Manson [4] developed empirical models based on the non-dimensional parameter l/D_h and Re, where D_h is the hydraulic diameter. However, their database consisted of non-offset-strip fin geometries: scaled-up and actual offset-strip fins, louvered fins, and finned flat tubes. Kays and London [3] made one of the first attempts to model the heat transfer and friction loss in offset-strip fins analytically and proposed a modified laminar boundary layer solution that includes the form-drag contribution of the blunt fin edges.

Wieting [5] developed several empirical correlations based on experimental data of flow friction and heat transfer for 22 configurations of offset-strip fin heat exchangers. Correlations were proposed for evaluating the f and j factors by extrapolation. However, the estimations from these correlations do not yield good predictions in the transition region. To overcome the problem of poor predictions in the transition regime, Joshi and Webb [6] proposed empirical correlations for estimating f and j for different hydraulic diameters that were not considered by Wieting [5]. They considered the effect of fin thickness, spacing, and length as well as the effect of the fin ends. They predicted the transition point by deriving the equation of Re^* given in Table 1 from the data sets of Kays and London [3], London and Shah [19], and Walters [20].

Mochizuki and Yagi [7] further improved Wieting's correlation by developing two sets of correlations for f and j factors, as shown in Eqs. (20)-(23) for Re < 2000 and $Re \geq$ 2000 based on Wieting's original correlation. Dubrovsky and Vasiliev [8] performed experimental investigations on 11 interrupted surfaces in a rectangular duct (offset-strip fin cores) without considering the burrs and bends on the edges of the fins. Only laminar and turbulent flow regions were examined, as done in the study of Mochizuki and Yagi [7]. They proposed empirical correlations for the Nusselt number and Darcy friction factors as shown in Eqs. (24)-(29), along with the correlation equations of the limiting Reynolds numbers used in the proposed equations for estimating these factors.

In this paper, an empirical formula developed by Manglik and Bergles [9] was selected as the reference model for comparing the accuracy and prediction range with those of the ANN-based model. Moreover, Eqs. (30) and (31) (see Table 1) given by Manglik and Bergles [9] are commonly used empirical formulas expressed by single equations for f and j, respectively, and they cover a wider prediction range with higher accuracy, compared with the other empirical formulas listed in Table 1.

Fig. 2 shows the accuracy of the empirical model developed by Manglik and Bergles [9]. Using the first experimental datasets in the range of 120 < Re <10^4, 0.134 < α (dimensionless fin height) < 0.997, 0.012 < δ (dimensionless fin length) < 0.048, and 0.041 < γ (dimensionless fin width) < 0.121, the empirical model was evaluated. Eqs. (30) and (31) in Table 1 show good correlation within ±20 % of the experimental data in references [19-23], as seen in the scatter plots in Fig. 2.

Fig. 3 shows the design process of the heat exchanger. First, the required parameters such as pressure drop and heat transfer rate should be determined for an application. Next, the heat exchanger type should be determined according to the operating conditions. Thereafter, design parameter sets should be determined. For example, α, δ, γ, and Re are the design parameter set for the offset-strip fin heat exchanger, as shown in Eqs. (30) and (31) in Table 1. For the given design parameter set, the heat exchanger performances can be estimated and rated based on the prediction model. To estimate and rate the

Table 1. Empirical models for offset-strip fin heat exchangers (continue).

Sl. No.	Authors	Data source	Database type	Correlation
01	Kays and London [3]	Analytical model for purely laminar boundary layer over interrupted plate surface.	Analytical model	$j = 0.665\, Re_l^{-0.5}$ (5) $f = 0.44(t/l) + 1.328 Re_l^{-0.5}$ (6)
02	Manson. [4]	Norris and Spofford [22], three offset-srip fin cores; Joyner [23], four scaled-up cores; London and Ferguson [21], one louvered fin core and one finned flat tube core.	Exp.	$j = \begin{cases} 0.6\left(\dfrac{l}{D_h}\right)^{0.5} Re^{0.5}, & \dfrac{l}{D_h} \le 3.5 \\ 0.321 Re^{0.5}, & \dfrac{l}{D_h} > 3.5 \end{cases}$ (7) For Re ≤ 3500: $f = \begin{cases} 11.8(l/D_h) Re^{0.67}, & l/D_h \le 3.5 \\ 3.371 Re^{0.67}, & l/D_h > 3.5 \end{cases}$ (8) For Re > 3500 $f = \begin{cases} 0.38(l/D_h) Re^{0.24}, & l/D_h \le 3.5 \\ 0.1086 Re^{0.24}, & l/D_h > 3.5 \end{cases}$ (9) where the hydraulic diameter is defined by $D_h = 2sh/(s+h)$
03	Wieting [5]	Kays and London [3], ten cores; London and Shah [19], nine cores; Walters [20], two cores; London and Ferguson [21], one louvered fin core.	Exp.	Re ≤ 1000 : $j = 0.483(l/D_h)^{-0.162} \alpha^{-0.184} Re^{-0.536}$ (10) $f = 7.661(l/D_h)^{-0.384} \alpha^{-0.092} Re^{-0.712}$ (11) Re ≥ 2000 : $j = 0.242(l/D_h)^{-0.322} (t/D_h)^{-0.089} Re^{-0.368}$ (12) $f = 1.136(l/D_h)^{-0.781} (t/D_h)^{-0.534} Re^{-0.198}$ (13) where $D_h = 2sh/(s+h)$.
04	Joshi and Webb [6]	Kays and London [3], 18 cores London and Shah [19], one core; Waters [20], two cores;	Exp.	$\mathrm{Re} \le \mathrm{Re}^*$ $j = 0.53(l/D_h)^{-0.15} \alpha^{-0.14} Re^{-0.5}$ (14) $f = 8.12(l/D_h)^{-0.41} \alpha^{-0.02} Re^{-0.74}$ (15) $\mathrm{Re} \ge \mathrm{Re}^* + 1000$ $j = 0.21(l/D_h)^{-0.24} (t/D_h)^{-0.02} Re^{-0.40}$ (16) $f = 1.12(l/D_h)^{-0.65} (t/D_h)^{-0.17} Re^{-0.36}$ (17) where $\mathrm{Re}^* = 257(l/s)^{1.23} (t/l)^{0.58} D_h \left[t + 1.328(Re/lD_h)^{-0.5}\right]^{-1}$ (18) and $D_h = 2(s-t)h/\left[(s+h) + th/l\right]$. (19)
05	Mochizuki and Yagi [7]	Experimental data for five scaled-up offset-strip fin cores [7]	Exp.	$\mathrm{Re} < 2000$: $j = 1.37(l/D_h)^{-0.25} \alpha^{-0.184} Re^{-0.67}$ (20) $f = 5.55(l/D_h)^{-0.32} \alpha^{-0.092} Re^{-0.67}$ (21) $\mathrm{Re} \ge 2000$: $j = 1.17(l/D_h + 3.75)^{-1} (t/D_h)^{0.089} Re^{-0.36}$ (22) $f = 0.83(l/D_h + 0.33)^{-0.50} (t/D_h)^{0.534} Re^{-0.20}$ (23) where $D_h = 2sh/(s+h)$.
06	Dubrovsky and Vasiliev [8]	Eleven cores in a double sand-wich arrangement but without splitter plate, which leaves a leakage path between top and bottom rows of strip fins. Kalinin et al. [24] non rectangular offset strip fin geometries	Exp.	$\mathrm{Re} \le \mathrm{Re}_{lim}$: $\mathrm{Nu} = 0.000437(l/D_h)^{-0.15} (t/D_h)^{-2.6} Re^x$ (24) where $x = 2.2(l/D_h)^{-0.02} (t/D_h)^{0.55}$ $\mathrm{Re} \ge \mathrm{Re}_{lim}$: $\mathrm{Nu} = 0.00723(l/D_h)^{-0.9} (t/D_h)^{-1.6} Re^x$ (25) where $x = 1.2(l/D_h)^{0.15} (t/D_h)^{0.34}$ $\mathrm{Re} \le \mathrm{Re}_{lim}$: $\xi = 1.05(l/D_h)^{-0.217} (t/D_h)^{-1.05} Re^x$ (26)

Table 1. (Continued).

Sl. No.	Authors	Data source	Database type	Correlation
06				where $x=-0.277\left(l/D_h\right)^{0.064}\left(t/D_h\right)^{-0.285}$ $Re_{lim}=3960\left(t/D_h\right)^{0.25}\left(l/D_h\right)^{0.42}$; (27) $\mathrm{Re}\geq\mathrm{Re}_{lim}$: $\xi=0.131\left(l/D_h\right)^{-0.234}\left(t/D_h\right)^{-0.44}Re^{x}$ (28) where $x=-0.0042\left(l/D_h\right)^{0.39}\left(t/D_h\right)^{-0.44}$, and $\mathrm{Re}_{lim}=448\left(l/D_h\right)^{0.09}\left(t/D_h\right)^{-0.653}$ (29)
07	Manglik and Bergles [9]	Kays and London [3] 15 cores London and Shah [21] 1 core Walters [19] 2cores	Exp.	$j=0.6522Re^{-0.5403}\alpha^{-0.1541}\delta^{0.1499}\gamma^{-0.0678}\times\left[1+5.269\times10^{-5}Re^{1.340}\alpha^{0.504}\delta^{0.456}\gamma^{-1.055}\right]^{0.1}$ (30) $f=9.6243Re^{-0.7422}\alpha^{-0.1856}\delta^{0.3053}\gamma^{-0.2659}\times\left[1+7.669\times10^{-8}Re^{4.429}\alpha^{0.920}\delta^{3.767}\gamma^{0.236}\right]^{0.1}$ (31) where, $0.129\leq\alpha\leq1.185, 0.012\leq\delta\leq0.06, 0.038\leq\gamma\leq0.214$

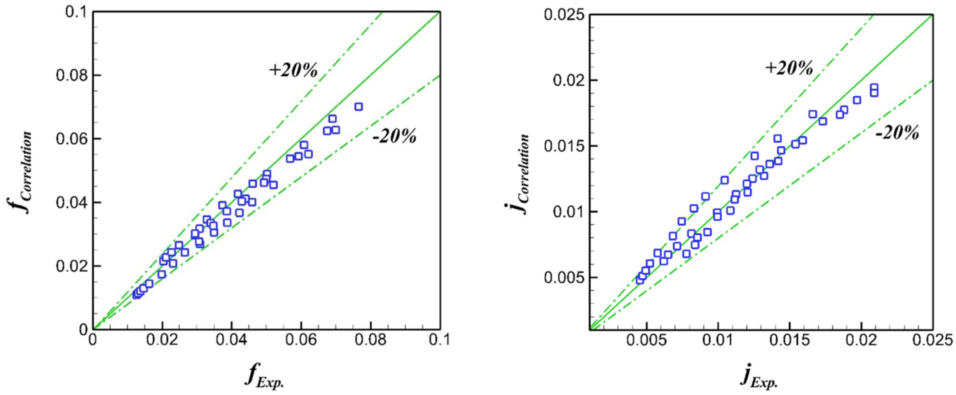

(a) (b)

Fig. 2. Comparison between the correlation and experimental data for offset-strip fin cores: (a) fanning friction factor *f*, (b) colburn factor *j*.

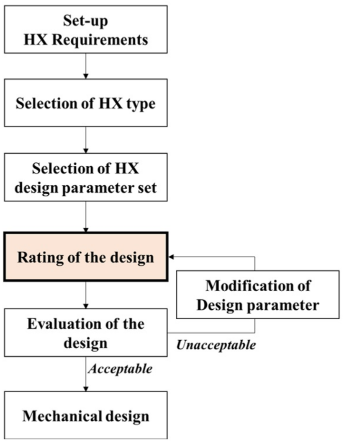

Fig. 3. Procedure for the design of a heat exchanger.

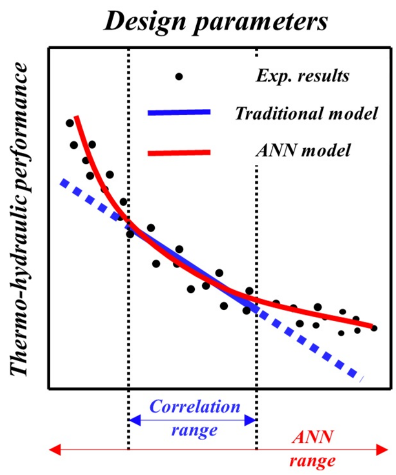

Fig. 4. Improved prediction range of the artificial neural network (ANN).

heat exchanger performances, prediction models such as empirical models or ANN models can be applied in the case of offset-strip fin heat exchangers. The rated heat exchanger designs are evaluated based on structural characteristics, manufacturability, etc. If the evaluations are unacceptable, the design parameters should be modified, and thermo-hydraulic performances should be re-rated until the evaluation results are acceptable.

Fig. 4 shows a conceptual diagram for improving prediction range using the ANN model. Previous prediction models have limitations in prediction range. In Fig. 4, the blue line represents the previous prediction model. An extrapolation is needed to predict the thermo-hydraulic performances in the ranges that are not covered by prediction models with relatively low accuracies, as recommended by Wieting [5]. This study considers an ANN model as an alternative to the previous prediction models. This ANN model is represented by a red line in Fig. 4 and it has a wider prediction range than the traditional prediction models and predicts the experimental results well. An ANN model can also be applied to the heat exchanger design process to evaluate the heat exchanger design and optimize the process.

2.3 Datasets on thermo-hydraulic performance for heat exchangers

Fig. 5 shows the flow chart of ANN model development for predicting the thermo-hydraulic performances of offset-strip fin heat exchangers. A typical ANN model development process involves six steps. The first process is the selection of the heat exchanger. In this study, offset-strip fin-type heat exchangers were selected. The second step is data gathering. To train the ANN model, experimental results and correlation data from the previous studies were used as the initial datasets. The third step involves preprocessing for the ANN model. Datasets were initially shuffled before training to reduce variance and ensure the generality of the model. The hyperparameters test is conducted to avoid the overfitting issues. Shuffled datasets were split into training data, validation data, and test data. Training data were used to train the ANN model and update weight and bias factors. The validation data were used to evaluate the given ANN model. The model was indirectly retuned based on the evaluation using the validation dataset. Test data were used for the unbiased evaluation of the final model fit on the training dataset. Hyperparameter tests were performed after data splitting. All the hyperparameters that can affect the ANN model were considered. In the hyperparameter tests, the design parameter, activation function, learning rate, steps, number of neurons, and number of layers were examined. Table 2 lists the hyperparameters used in the present ANN model. The input and output parameters were determined based on related previous studies. The rectified linear unit (ReLU) activation function [18] was adopted in the present ANN model. To determine the number of hidden layers, the number of neurons in the hidden layer, learning rate, steps, etc., additional tests such as the neuron dependency test were conducted. The fourth step in the typical ANN model development process is data learning. In the present study, a 1-layer ANN model was con-

Table 2. Hyperparameters of the artificial neural network (ANN).

Parameter/method	Value
Input parameter	α, δ, γ, Re
Output parameter	f, j
Activation function	Rectified linear unit (RELU) $y = f(x) = \begin{cases} 0 & \text{for } x < 0 \\ x & \text{for } x \geq 0 \end{cases}$
Number of neurons in a hidden layer	25
Number of layers	3
Learning rate base	0.2
Learning rate decay	0.99
Decay steps	400
Regular rate	0.001
Total steps	80000

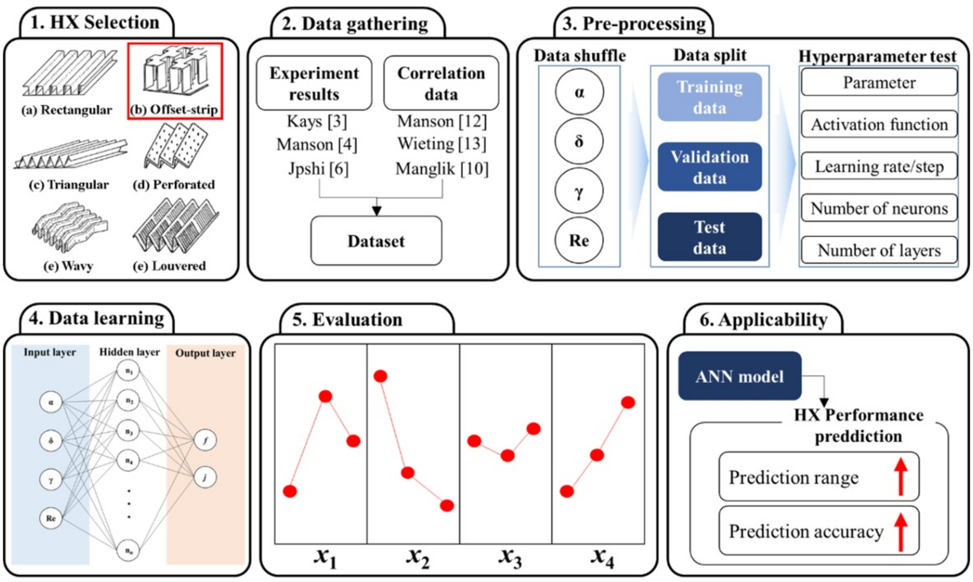

Fig. 5. Flow chart of ANN model development for predicting the thermohydraulic performances of offset-strip fin heat exchangers.

sidered to predict the thermo-hydraulic performances of offset-strip fin heat exchangers according to the hyperparameter test. Dimensionless parameters α, δ, γ, and Re were taken as the input parameters, and f and j as the output parameters. The fifth step is the evaluation of the ANN model. The accuracies and prediction ranges of the ANN model were evaluated. Additionally, each input parameter was also evaluated to understand the influence of the input parameters on the thermo-hydraulic performance. Based on the findings of the evaluation step, the applicability of the ANN model is examined in the final step.

An ANN model comprises artificial neurons, which are linked together according to the specific network architecture. The neural networks can transform the inputs into the outputs without any background information. All neurons in one layer are connected to those in the next layer, with variable weights and bias values, which are generally assigned random initial values. Learning data can be setup in the input layer and passed on to the hidden layer through the weighted connections. Subsequently, the neurons in the hidden layer sum the processed data to determine the output layers.
The final output can be represented as follows:

$$y = \phi\left[\phi\left(W^1 x + B^1\right)W^2 + B^2\right]. \quad (32)$$

Here, x and y are the scaled input and output vectors, respectively. W and B represent the weight and bias of each neuron, respectively. Superscript 1 represents the connection value between the input and hidden layers, and superscript 2, the connection value between the hidden and output layers. y is the activation function based on ReLU and is defined as follows:

$$y = \phi(x) = \begin{cases} 0\, for x < 0 \\ x for x \geq 0. \end{cases} \quad (33)$$

Fig. 6 shows a block diagram of an ANN algorithm for predicting the thermo-hydraulic performance of the offset-strip fin heat exchanger. Datasets are shuffled for random training and divided into three parts: training data, validation data, and test data. The initial W and B values are generated based on the

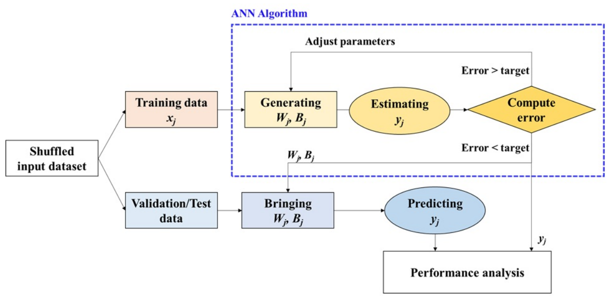

Fig. 6. Block diagram for the ANN algorithm.

training data. Using Eq. (32), the output variable y can be calculated with the initial W and B. If the error is higher than the target value when the reference value is compared with the estimated value y, W and B values are modified, and the processes are repeated until the error is reduced to the target value. When the error meets the target value, W and B values are applied to validate the ANN algorithm. The validation data and test data do not participate in the training of the ANN algorithm; they are used for checking the accuracy of the ANN algorithm.

The ANN algorithm for training a back-propagation network involves the following steps:

1) Select variables and prepare datasets.

2) Decide the number of neurons and initialize weights and bias as random values.

3) Present input X and desired output O.

4) Propagate feed-forward (input and hidden layers).

5) Calculate the actual output values,

$$O_k = \phi\left(\sum_{i=1}^{m} W_{kj} X_j + B_k\right) \quad (34)$$

where i and k represent the input layer and output layer neurons, respectively, and $\phi(x)$ is an activation function.

6) Evaluate the output layer error between the desired output and calculated output

$$\delta_k = O_k\left(1 - O_k\right)\left(Y - O_k\right) \quad (35)$$

where δ_k is the output layer error, and Y is the desired output value.

7) Adjust the weights and bias values in the output and hidden layers

$$W_{kj(ji)}\left(t+1\right) = W_{kj(ji)}(t) + \alpha\delta_{k(i)} h_{j(i)} \eta \left[W_{kj(ji)}\left(t\right) - W_{kj(ji)}\left(t-1\right)\right] \quad (36)$$

$$b_{k(j)}\left(t+1\right) = b_{k(j)}\left(t\right) + \alpha\delta_{k(j)} \quad (37)$$

where α is the learning rate, and η is the momentum factor that allows the previous weight change to influence the weight change in this time period t.

8) Repeat steps (2)-(7) until the error of the output layer reaches specified tolerance.

In this study, the thermo-hydraulic performances depended on the dimensionless parameters α, δ, γ, and Re, as shown in Eqs. (30) and (31) in Table 1. To build the prediction model, these parameters can be characterized as input variables (x). The output value (y) is the thermo-hydraulic performance represented by f and j.

During the ANN algorithm training, the experimental results (y_{data}) are the known values. Hence, the ANN prediction results can be compared with the experimental results. The output error can be reduced by increasing the number of neurons in the hidden layer. In this study, the accuracy of the ANN and experimental results were compared in terms of the regression coefficient (R^2), root-mean-square error ($RMSE$), and root mean relative error ($RMRE$):

$$R^2 = 1 - \frac{\sum_{i=1}^{n}(y_{data} - y_{ANN})^2}{\sum_{i=1}^{n}(y_{data})^2} \quad (38)$$

$$RMSE = \sqrt{\frac{1}{n}\sum_{i=1}^{n}(y_{Data} - y_{ANN})^2} \quad (39)$$

$$RMRE = \sqrt{\frac{1}{n}\sum_{i=1}^{n}\left|\frac{y_{Data} - y_{ANN}}{y_{Data}}\right|}. \quad (40)$$

The optimum number of neurons was determined by comparing these three values to assure the accuracy and minimize the computing time. ANN analysis was performed using custom Python code.

3. Results and discussion

3.1 Neuron dependency test

Fig. 7 shows the results of the neuron dependency test for the ANN model. Overfitting, which is undesirable, may occur during the training process. In the present study, the number of data sets are limited. Thus, the number of neurons to be used in ANN algorithm should be optimized based on the neuron dependency test by comparing the R^2, $RMSE$, and $RMRE$ values for each number of neurons. The limited data sets were divided into training data, validation data, and test data as follows: 50 % of the data were used as training data; 25 % were used as validation data; the remaining 25 % were used as test data. Training data sets were used for generating and evaluating the ANN algorithm. Validation data sets were used for validating the process by comparing the results of the ANN model and experiments.

The averaged values of R^2, $RMSE$, and $RMRE$ for the training, validation, and test data were evaluated for the neuron dependency test. Normally, higher R^2 and lower $RMSE$ and $RMRE$ values mean that ANN model predictions of the thermo-hydraulic performances are more accurate than the experimental results. In Fig. 7, the fluctuation in R^2 values becomes stable for more than 12 neurons. Additionally, $RMRE$ and $RMSE$ values are almost constant when 25 neurons are chosen. Thus, in the present study, the number of neurons was set as 25 to minimize the computing cost and achieve higher accuracy without overfitting. As shown in Fig. 7(d), the minimum $RMRE$ values are obtained when learning rate is equal or larger than 0.2 and step size of 80000. Hence, a learning rate of 0.2 and step size of 80000 were chosen for the subsequent ANN modeling.

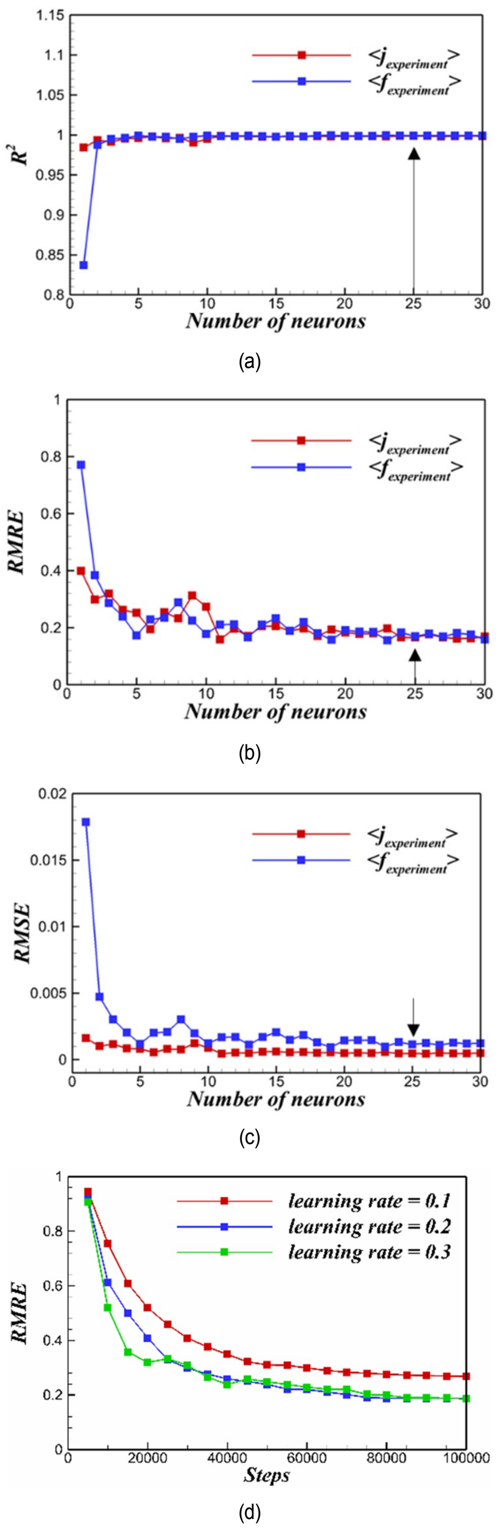

Fig. 7. Selecting the number of neurons in the hidden layer in the ANN model trained by experimental data: (a) regression coefficient; (b) root mean relative error; (c) root-mean-square error; (d) learning rate.

3.2 ANN model prediction using limited experiment data

The limited experimental data includes 44 experimental datasets for f and j of the offset-strip fin heat exchanger in the range $120 < Re < 10^4$, $0.134 < \alpha < 0.997$, $0.012 < \delta < 0.048$, and $0.041 < \gamma < 0.121$, which are available in Ref. [9]. Manglik

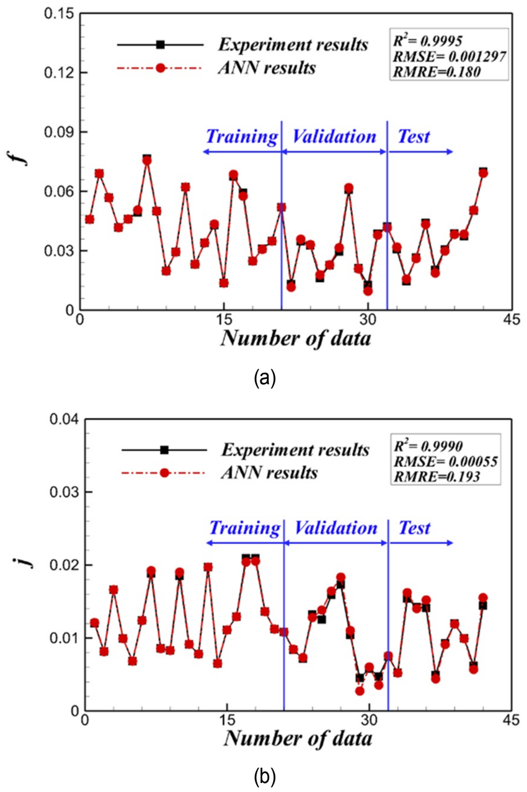

Fig. 8. One-step-ahead prediction output superimposed on experimental output using the ANN trained by experimental data in the applicable range: (a) *f*; (b) *j*.

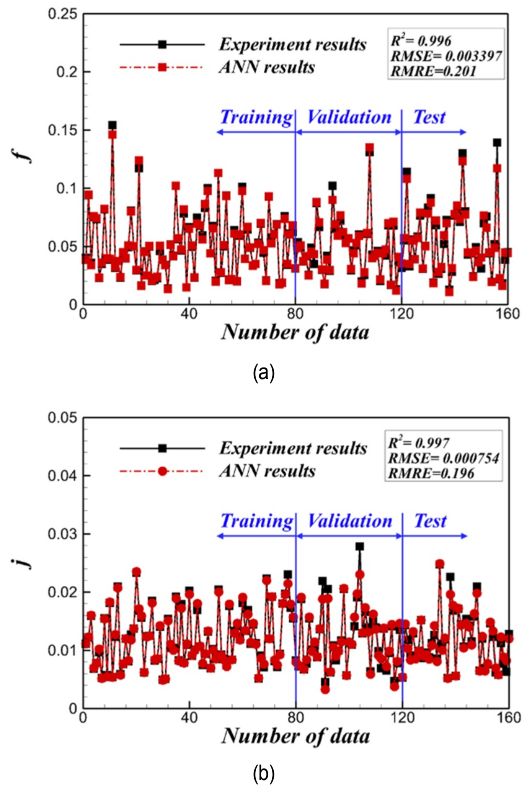

Fig. 9. One-step-ahead prediction output superimposed on experimental output using the ANN trained by experimental data in the expanded range: (a) *f*; (b) *j*.

and Bergles [9] used these datasets and derived empirical correlations for f and j for the offset-strip fin heat exchanger, as shown in Eqs. (30) and (31) in Table 1; these are the most commonly used correlations for f and j for the aforementioned input parameter range (Re, α, δ, and γ). As shown in Fig. 2, these empirical correlations predict f and j for the heat exchanger within ±20 % error for the limited application range of the input parameters. Therefore, for predicting the thermo-hydraulic performance of offset-strip fin heat exchangers, it is essential to improve the prediction accuracy and coverage of the input parameters using the ANN models compared to the empirical correlations [9]. For this purpose, the first training of the ANN model was conducted using datasets available in the limited range covered by Manglik and Bergles's model [9].

Fig. 8 shows the one step-ahead prediction output superimposed on the experimental output using ANN with limited experiment data for f and j; 44 experimental datasets were used for f and j each. To avoid underfitting or overfitting, the training, validation, and test data contained 22, 11, and 11 data, respectively, for each of f and j. The ANN results after training showed good agreement with the experimental results in terms of f and j. Additionally, after validation and testing, the differences between the ANN and experimental results were slightly larger than those after training. However, the averaged R^2 values were 0.9995 and 0.9990 for f and j, respectively, indicating the higher accuracy of the ANN predictions. Hence, the present ANN algorithm can be applied to predict the performance of offset-strip fin heat exchangers.

3.3 Prediction of ANN model using expanded experiment data

As mentioned earlier, the previous empirical correlations, i.e., Eqs. (30) and (31), were proposed for limited ranges of independent variables. However, with advances in manufacturing technology, thinner and smaller offset-strip fins have been developed. Hence, it is difficult to predict the thermo-hydraulic performances of offset-strip fin heat exchangers using the previous empirical correlations. Therefore, it is essential to derive correlations applicable for wider prediction ranges to estimate the thermo-hydraulic performances of small offset-strip fin heat exchangers more accurately. To that end, this study considered all the experimental datasets listed in Table 1, including those with wider prediction ranges beyond those applicable for Eqs. (30) and (31). This expanded experimental dataset in Table 1 was used to develop an ANN model that can accurately predict f and j over much wider prediction ranges of design parameters.

Fig. 9 shows the one-step-ahead prediction output superimposed on the experimental output trained by expanded experiment data for f and j. Overall, 160 datasets in Table 1 were used for ANN modeling. Similar to the limited experiment data-

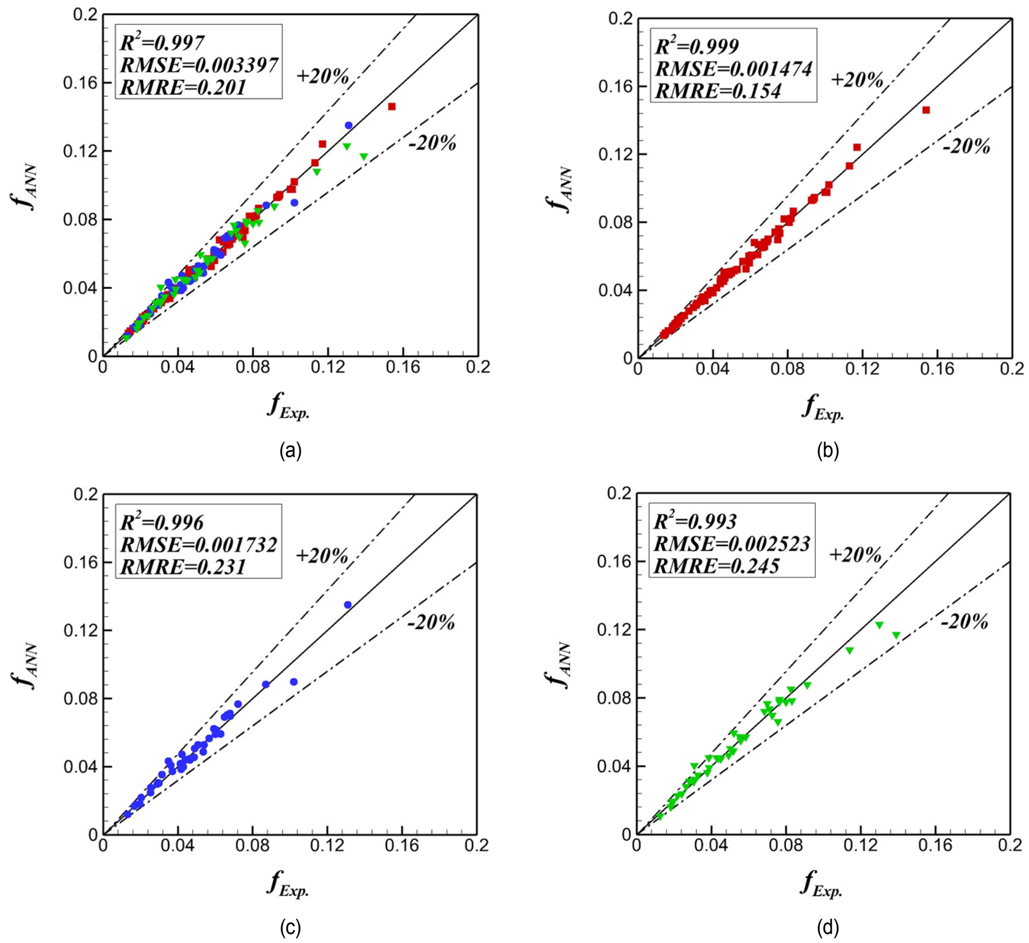

Fig. 10. Comparison of the experimental results obtained with the predictions from the ANN trained by the expanded experiment data for *f*: (a) total data; (b) training data; (c) validation data; (d) test data.

set, the initial datasets were divided into three parts: 50 % of the initial data sets were used as training data, 25 % as validation data, and the remaining 25 % as test data. The R^2 values for the total data sets were 0.996 (*f*) and 0.997 (*j*); the *RMSE* values were 0.003397 (*f*) and 0.000754 (*j*); the *RMRE* values were 0.201 (*f*) and 0.196 (*j*). The R^2 values for the expanded experimental dataset are lower than those for the limited experimental dataset. Similarly, the *RMSE* and *RMRE* values for the expanded experimental dataset are higher than those for the limited experimental dataset.

Fig. 10 shows a comparison of the ANN prediction results for f trained by the expanded experiment datasets of 160 data with the experimental results listed in Table 1 within the ±20 % error band. For the total, training, validation, and test datasets, the values of R^2 are 0.997, 0.999, 0.996, and 0.993, respectively; the values of *RMSE* are 0.003397, 0.001474, 0.001732, and 0.002523, respectively; the values of *RMRE* are 0.201, 0.154, 0.231, and 0.245, respectively. The weight and bias values for f and j are listed in Tables 3 and 4, respectively, for the present ANN model.

Fig. 11 shows a comparison of the ANN prediction results for j trained by the expanded experimental datasets of 160 with the experimental results listed in Table 1 within the ±20 % error band. For the total, training, validation and test datasets, the values of R^2 are 0.997, 0.999, 0.992 and 0.995, respectively; the values of *RMSE* are 0.000754, 0.000264, 0.000565, and 0.000423, respectively; the values of *RMRE* are 0.196, 0.141, 0.246, and 0.231, respectively.

Compared to the ANN predictions of f and j using the limited experimental data, those obtained using the expanded experimental dataset have smaller R^2 values and larger *RMSE* and *RMRE* values, showing a slight decrease in the prediction accuracy because of the wider coverage of the design parameters when using more experimental datasets. Thus, the present ANN-based model using the expanded experimental data can predict the thermo-hydraulic performances in offset-strip fin heat exchangers within ±20 % accuracy and cover much wider ranges of the design parameters than possible using the correlations in Eqs. (30) and (31).

3.4 Prediction of ANN model using expanded experiment data

Fig. 12 shows the effect of the design parameters *Re*, α, δ,

Table 3. ANN weight and bias values for *f*.

	$W_{j,1}$	$W_{j,2}$	$W_{j,3}$	$W_{j,4}$	$W_{1,j}$	$B_{1,j}$	B_2
1	-0.1130	-0.0060	-0.0840	-0.9610	0.9670	-0.4714	-0.5988
2	0.0670	-0.1540	0.1380	-0.0100	-0.2180	0.1217	
3	0.2170	0.0100	0.3120	-0.9720	1.0430	-0.8408	
4	0.0450	-0.1030	0.0920	-0.0070	-0.1460	0.0817	
5	0.1100	-0.2530	0.2260	-0.0160	-0.3580	0.2006	
6	-0.0520	0.0800	-0.1060	-1.1670	1.1760	-0.8405	
7	0.1090	-0.2540	0.2260	-0.0160	-0.3580	0.1992	
8	0.0420	0.0150	0.0210	0.0530	-0.0720	0.0051	
9	0.2980	0.0690	0.1830	-0.0130	0.3570	0.0420	
10	0.0640	-0.1490	0.1330	-0.0100	-0.2110	0.1170	
11	-1.3450	0.2510	0.0460	-0.0060	1.3700	-1.3438	
12	0.1840	0.0770	0.0770	0.2170	-0.3040	0.0179	
13	-0.2680	-0.4090	-0.2370	-0.5440	0.7680	-0.1881	
14	0.0670	0.2470	-0.1410	-2.0020	2.0210	-1.6019	
15	1.0800	0.2120	0.6130	-0.0050	-1.2610	-0.8907	
16	0.0980	0.0310	0.0550	0.1280	-0.1730	0.0136	
17	0.0560	-0.1310	0.1170	-0.0090	-0.1850	0.1025	
18	0.3300	-0.1180	-0.2290	-0.2250	-0.4770	-0.4242	
19	-0.1680	0.0910	-0.1580	-0.5370	0.5910	0.0163	
20	-0.0420	-0.0700	-0.1080	-0.0430	-0.1420	-0.0065	
21	0.7180	-0.0120	0.3830	-0.1440	0.8260	-0.1032	
22	0.2920	-0.0250	-0.2760	0.0490	-0.4050	-0.1658	
23	0.5290	0.1320	0.3290	-0.0100	0.6370	0.0897	
24	0.0610	-0.1420	0.1270	-0.0090	-0.2010	0.1122	
25	0.0670	0.0550	-0.0580	-0.8110	0.8240	-0.4301	

Table 4. ANN weight and bias values for *j*.

	$W_{j,1}$	$W_{j,2}$	$W_{j,3}$	$W_{j,4}$	$W_{1,j}$	$B_{1,j}$	B_2
1	0.0173	-0.0338	0.0048	0.0179	-0.0420	-0.0068	-0.0598
2	0.0209	-0.1400	0.0459	0.2682	-0.3045	0.1599	
3	-0.7585	0.2153	0.1200	0.1748	0.8149	-0.9266	
4	0.0555	-0.1550	0.0262	0.2121	-0.2699	0.0831	
5	-0.0101	-0.0959	-0.0156	0.2648	0.2819	0.0538	
6	0.0467	-0.4681	-0.0471	0.4544	-0.6559	0.2090	
7	-0.0965	0.0775	-0.1268	-0.6010	0.6263	-0.2237	
8	0.2114	-0.4866	-0.4407	-0.0546	-0.6896	-0.6443	
9	0.0919	0.2994	0.0935	-0.5928	0.6770	-0.0916	
10	-0.2938	0.0954	-0.0853	0.2468	-0.4044	0.3899	
11	-0.3683	-0.1564	-0.2554	-0.1864	0.5099	0.0320	
12	0.1837	0.1325	-0.0697	-2.1182	2.1313	-1.5573	
13	0.0082	-0.0695	-0.0056	0.0386	-0.0799	-0.0128	
14	-0.1414	-0.0092	-0.4552	0.3544	0.5962	0.3247	
15	0.0070	-0.0875	0.2842	0.0426	-0.3006	-0.0206	
16	0.1954	-0.0277	-0.1741	-0.7057	0.7540	-0.3958	
17	0.0041	-0.0509	0.1653	0.0248	-0.1747	-0.0120	
18	0.0038	-0.0324	-0.0026	0.0180	-0.0373	-0.0060	
19	-0.3602	0.1552	0.1454	0.6080	0.7376	-0.0098	
20	0.0613	-0.0149	0.1104	-0.0709	0.1415	-0.0974	
21	-0.2252	0.0448	0.0861	0.0561	-0.2547	0.1987	
22	-0.4795	0.1556	-0.1394	0.4028	-0.6599	0.6363	
23	-0.0193	0.2921	-0.1687	-0.9517	1.0095	-0.3733	
24	-0.3231	0.0643	0.1236	0.0805	-0.3654	0.2852	
25	-0.7631	0.1735	0.0649	-0.2902	0.8358	-0.6546	

and γ on f. In the figure, the black, red, and blue symbols represent the f obtained from experiments, predicted by correlations Eqs. (30) and (31), and predicted by the present ANN model, respectively. Fig. 12(a) shows the effect of Re on f. An inverse relationship is observed between Re and f. This relationship is attributed to the negligible viscous losses at higher Re compared to inertia forces. Consequently, the viscous losses decreased with decreasing f. Additionally, the recirculation zones formed beyond the fin-offset area, decreasing the pressure drop effect in the offset region. The predictions of f based on the correlations are within a considerably limited range of Re, as shown in Fig. 12(a). In contrast, the present ANN model can predict the f factor over relatively wide ranges of Re. Owing to the limitations associated with the prediction range, the predictions from the correlation in the chosen range of Re ($120 < Re < 10^4$) were not accurate.

In case of the geometrical parameters (α, δ, and γ), their values represented in the datasets used for ANN model were changed simultaneously. Therefore, the exact relationship, as in the case of the relation between f and Re could not be investigated. However, the trend between the geometrical parameters and f was interpreted. Fig. 12(b) shows the general effect of α on f. In general, there exists an inverse relationship between α and Re. A higher value of α indicates that the frontal cross section of the offset-strip fin is large, and hence, the frictional loss is low.

Fig. 12(c) shows the effect of δ on f. Initially, the boundary layer grows across the offset-strip fin surface, and subsequently, it is disrupted at the end of the offset-strip fin. Essentially, for flows over short fins of finite thicknesses, there is an outward displacement of the boundary layer near the leading edge of the offset-strip fin, followed by a local acceleration near the trailing edge, and eventual dissipation in the fin wakes. Hence, higher values of δ result in high f, eventually increasing the pressure drop in offset-strip fin heat exchanger.

Fig. 12(d) shows the effect of γ on f. The γ values represent the ratio of fin thickness to fin width within an offset-strip fin. Thicker fins have larger form drag at the leading edge, and hence, the passages are smaller for smaller fin density. There is a consequent reduction in the free-flow area. Therefore, the pressure drop through offset-strip fin increases as γ value increases.

Fig. 13 shows the effect of the design parameters on j factor. Similar to Fig. 12, the black, red, and blue symbols in Fig. 13 represent j obtained from experiments, correlation, and ANN, respectively. Fig. 13(a) shows the effect of *Re* on j. According

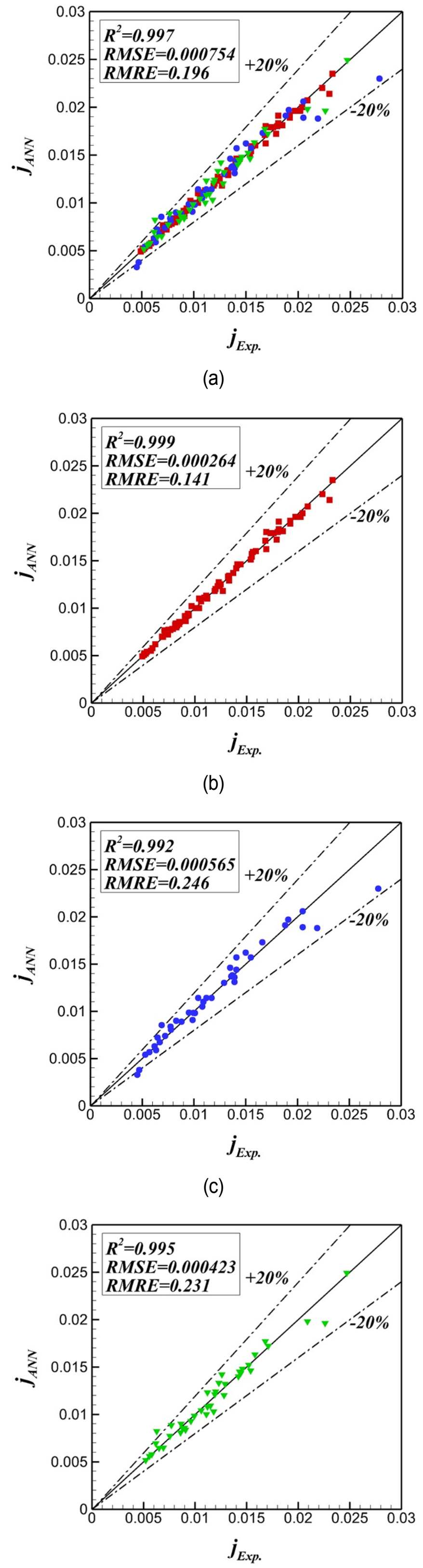

Fig. 11. Comparison of the experimental results obtained with the predicted results from the ANN trained by the expanded experiment data for *j*: (a) total data; (b) training data; (c) validation data; (d) test data.

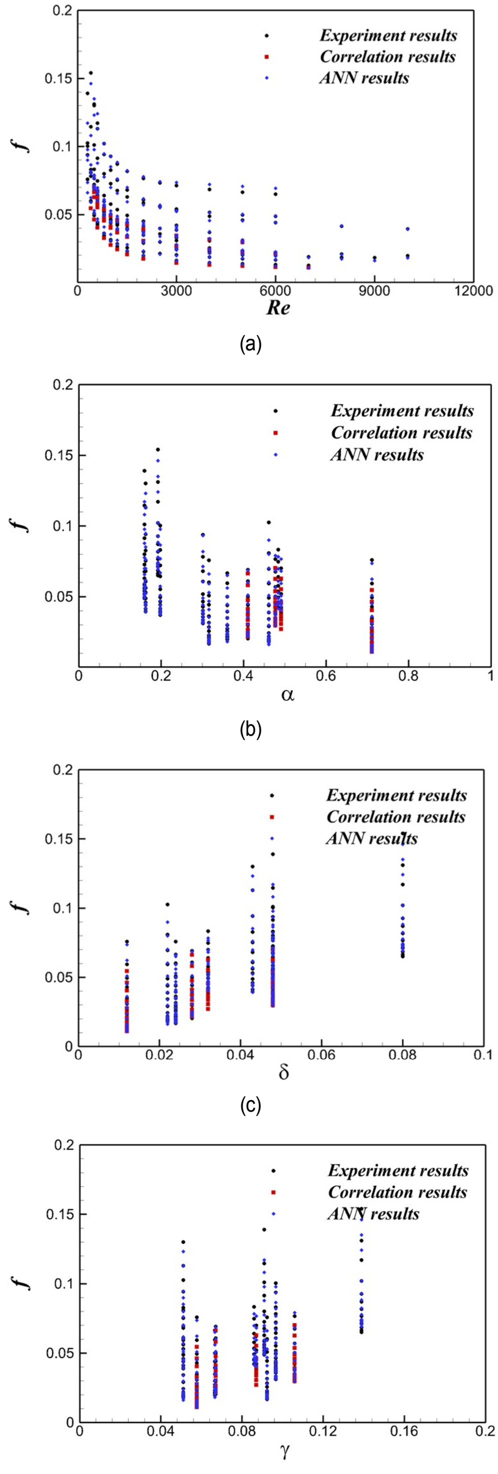

Fig. 12. Effect of the design parameters on the Fanning friction factor *f*: (a) *Re*; (b) *α*; (c) *δ*; (d) *γ*.

to Fig. 13(a), an inverse relationship exists between *Re* and *j*. Local recovery zones decreased as *Re* increased with the formation of small recirculation zones, as reported by Manglik and Bergles [9]. Thus, the heat transfer performance diminished at the leading edge of the offset-strip fin. The predictions of *j*

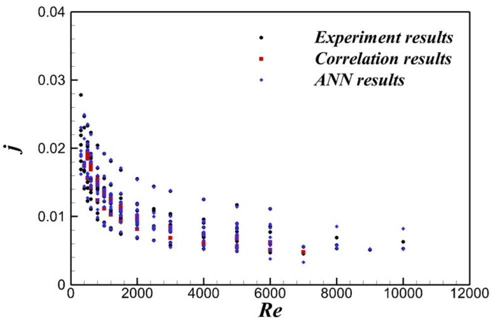

(a)

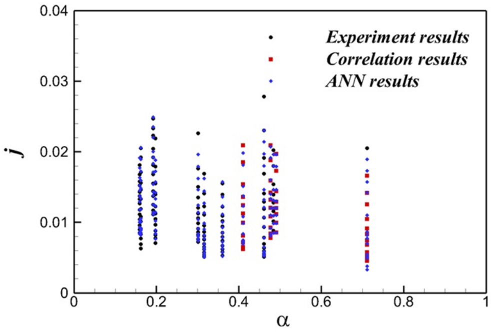

(b)

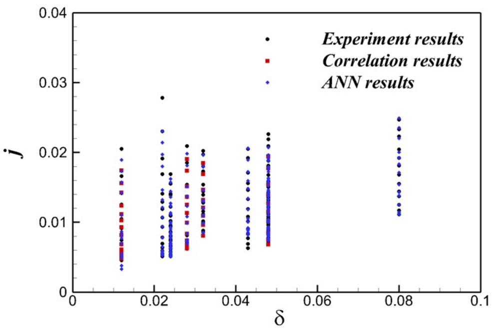

(c)

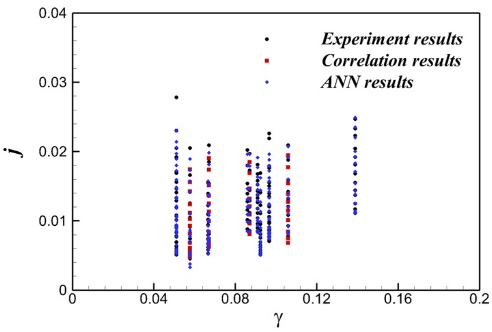

(d)

Fig. 13. Effect of the design parameters on the Fanning friction factor j: (a) Re; (b) α; (c) δ; (d) γ.

based on the correlations are within a considerably limited range of Re, as seen in Fig. 13(a). In contrast, the present ANN-based model predicts j over relatively wide ranges of Re. Similar to the case of f, owing to the limitations associated with the prediction range, the predictions from the previous correlation beyond the range of *Re* ($120 < Re < 10^4$) were not accurate.

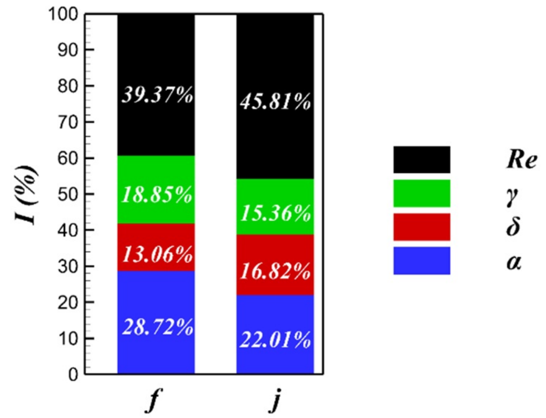

Fig. 14. Relative impact of the design parameters on the performance of the offset-strip fin heat exchanger.

As mentioned earlier, the parameters α, δ, and γ in the datasets used for ANN model were changed simultaneously, and hence, the relationship between them and j can not be clearly evaluated; however, the rough trend between them and j are shown in Figs. 13(b)-(d). Fig. 13(b) shows the effect of α on j. In general, there exists an inverse relationship between α and j. A higher α indicates a larger frontal cross-sectional area of the offset-strip fin. For offset-strip fins with relatively wide cross sections, the local recovery zone with flow-mixing effects decreases in the free stream layer. Consequently, the heat transfer performance is slightly diminished. Moreover, the ANN predicts j over a wide range of α unlike the correlation-based predictions, which are limited to a high range of α.

Fig. 13(c) shows the effect of δ on j. Initially, the thermal boundary layer grows through the offset-strip fin surface, and subsequently the boundary layer is disrupted at the end of the offset-strip fin. Essentially, for the flow over short lengths of fins of finite thicknesses, there is an outward displacement of the boundary layer near the leading edge of offset-strip fin, followed by a local acceleration near the trailing edge, and eventual dissipation of the boundary layer in the fin wakes. Additionally, the regrowth of the thermal boundary layer at the leading edge of the offset-strip fin can remarkably affect the heat transfer perfor mance of the offset-strip fin heat exchangers. Hence, higher values of δ result in higher j values, eventually enhancing the heat transfer performance of the offset-strip fin heat exchanger.

Fig. 13(d) shows the effect of γ on j. Thicker fins form a secondary vortex at the trailing edge of the offset-strip fin, resulting in smaller passages with smaller fin density. There is a consequent reduction in the free-flow area. Therefore, the heat transfer performance of the offset-strip fin is enhanced as γ increases.

Fig. 14 shows the relative impact of the input variable on the design parameters of the heat exchanger. The physical parameters, which are related to thermo-hydraulic performance of the offset-strip fin heat exchanger, are widely known. However,

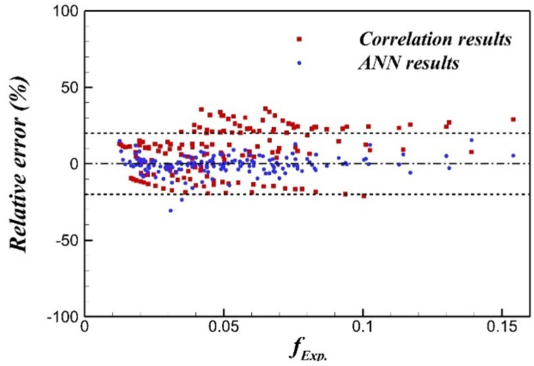

(a)

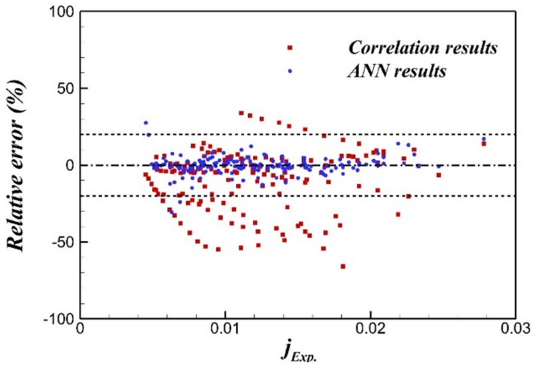

(b)

Fig. 15. Comparison the relative errors between the correlation results and ANN results: (a) *f*; (b) *j*.

the relative impact of these design parameters on the thermo-hydraulic performance is unclear. In the ANN model, the effect of each input parameter on the output variables can be calculated in terms of the weight and bias values in ANN algorithms. To calculate the relative impacts, Garson's model was applied:

$$I_i = \frac{\sum_{f=1}^{j=h}\left(\left(\frac{W_{j,i}^{f,i}}{\sum_{i=1}^{i=5}\left|W_{j,i}^{1}\right|}\right)\bullet\left|W_{1,j}^{2}\right|\right)}{\sum_{i=1}^{i=5}\left\{\sum_{j=1}^{j=n}\left(\frac{W_{j,i}^{1}}{\sum_{i=1}^{i=5}\left|W_{j,i}^{1}\right|}\right)\bullet\left|W_{1,j}^{2}\right|\right\}} \tag{41}$$

where n, I_i, W^1_{ji}, and W^2_{ij} are the number of neurons in the hidden layer, the relative impact of the i^{th} input factor, the weight signal from i^{th} neuron in the input layer to the i^{th} neuron in the hidden layer, and the weight signal from the i^{th} neuron in the hidden layer to the i^{th} neurons in the output layer, respectively. As shown in Fig. 14, the thermo-hydraulic performance of the offset-strip fin heat exchanger strongly depends on the Reynolds number: 39.37 % and 45.81 % for f and j, respectively. The second dominant input parameter is the dimensionless fin height with relative impacts of 28.72 % and 22.01 % for f and j, respectively. The relative impacts of γ and δ for f are 18.85 % and 13.06 %, respectively, while those for j are 15.36 % and 16.82 %, respectively. Thus, the Reynolds number has the largest impact on f and j. The parameters that have the smallest impact on f and j are δ and γ, respectively. As shown in Fig. 14, the design parameters, Re, α, δ, and γ, influence the thermo-hydraulic performance of the offset-strip fin heat exchanger through their effects on f and j.

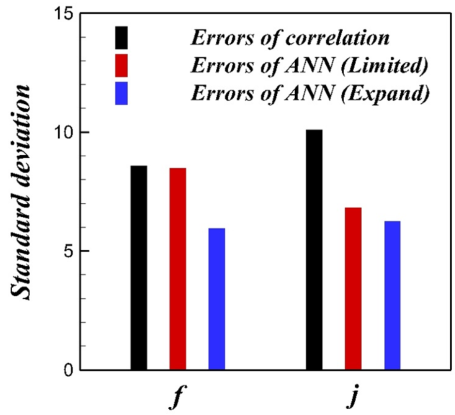

Fig. 16. Standard deviations of the relative errors.

Fig. 15 shows the relative errors in f and j predicted by the present ANN model and using correlations in Eqs. (30) and (31) within the ±20 % error band compared to the experimental results. The relative errors of f and j predicted by the previous correlations are widely dispersed from the centerline and widely distributed in the range beyond the ±20 % band. However, the relative errors of f and j predicted by the ANN model are generally within the ±20 % band range and are distributed along the centerline, except for a few points corresponding to Reynolds number less than 100. The maximum relative errors for f and j predicted by previous correlations are +41 % and –73 %, respectively, which are much larger compared to those for the present

ANN model predictions. The previous correlations tend to overestimate f and underestimate j, as shown in Fig. 15. However, the maximum relative errors of f and j factors predicted by the ANN-based model are –32 % and –33 % for f and j, respectively, which are observed at a few points corresponding to Reynolds numbers less than 100. Thus, the present ANN model yields results with a prediction accuracy of ±20 %, and it is a suitable alternative for the previous correlations [9] and is capable of predicting the thermo-hydraulic performance based on f and j more accurately over a wider range.

Fig. 16 shows the standard deviations of the relative errors, σ_{err}, for f and j predicted by previous correlations and by the present ANN-based models using the limited and expanded experimental data. For f, the values of σ_{err} predicted by the correlation in Eq. (30) and the ANN-based model using the limited and expanded experimental data are 8.58, 8.48, and 5.95, respectively. Similarly, the values of σ_{err} for j predicted by the correlation in Eq. (31) and the ANN-based model using the limited and expanded experimental data are 10.01, 6.83, and 6.24, respectively. Thus, we can observe a larger decease in the σ_{err} values predicted by the ANN-based model using the expanded experimental data compared to those predicted by the correlations in Eqs. (30) and (31).

4. Conclusions

An ANN model was proposed to improve the prediction accuracy and range for thermo-hydraulic performance prediction for an offset-strip fin heat exchanger. The ANN model was trained using the experimental dataset reported by Kays and London [3]. For ANN training, dimensionless geometrical parameters α, δ, and γ and Reynolds number (Re) were selected as the input variables and f and j were represented as the output variables. The prediction results of ANN model were compared with those of Manglik and Bergles's model [9].

The ANN prediction based on Manglik and Bergles's model was conducted within a limited input parameter range. The ANN models predicted Kays and London's experimental data very well, showing a higher accuracy than that of Manglik and Bergles's model. The prediction results for the limited input parameter range showed the applicability of ANN model in predicting the thermo-hydraulic performance of the offset- strip fin heat exchanger.

To improve the prediction range, ANN predictions were obtained for an expanded input parameter range that can not be covered by Manglik and Bergles's model. Sensitivity analysis for the thermo-hydraulic performance of the offset-strip fin heat exchanger was also performed using the ANN model. The maximum relative errors for f and j as predicted by previous correlations were much larger than those of the present ANN model predictions. Moreover, the standard deviations of the relative errors for the previous correlations were much larger. The relative impacts of the input variables on the design parameters of the heat exchanger were evaluated. The Reynolds number has the largest impact on f and j. The proposed ANN model can explain how the input parameters influence the thermo-hydraulic performance of the offset-strip fin heat exchanger.

Acknowledgments

This research was partly supported by the National Research Foundation of Korea (NRF) grant funded by the Korea government (MSIT) [NRF-2019R1A5A8083201]. This work was partly supported by Korea Institute of Energy Technology Evaluation and Planning (KETEP) grant funded by the Korea government (MOTIE) (20193310100050, Technology development of gas turbine blade reengineering specialized for domestic operating environment).

Nomenclature

Symbols

B : Bias vector
c_p : Specific heat
D_h : Hydraulic diameter of fin
f : Fanning friction factor
j : Colburn factor
G : Mass flux
h : Fin height
I : Relative impact
l : Fin length
Pr : Prandtl number
q : Heat flux
t : Fin thickness
R^2 : Coefficient of regression
Re : Reynolds number
$RMRE$: Root mean relative error
$RMSE$: Root-mean-square error
St : Stanton number
T : Temperature
w : Fin width
W : Weight

Greek symbols

α : Dimensionless fin height
β : Thermal expansion coefficient
δ : Dimensionless fin length
γ : Dimensionless fin width
σ_{err} : Standard deviation for relative error
τ : Wall shear stress
λ : Thermal conductivity
μ : Dynamic viscosity
ρ : Density

Sub/superscripts

w : Wall
m : Average

References

[1] K. H. Do, B. Choi, Y. Han and T. Kim, Experimental investigation on the pressure drop and heat transfer characteristics of a recuperator with offset strip fins for a micro gas turbine, *International Journal of Heat and Mass Transfer*, 103 (2016) 457-467.
[2] Y. Yin, X. Zhang, G. Wang and L. Luo, Experimental study on a new internally cooled/heated dehumidifier/regenerator of liquid desiccant systems, *Intenational Journal of Refrigeration*, 31 (2008) 857-866.
[3] W. M. Kays and A. L. London, *Compact Heat Exchangers*, 3rd Ed., New York (1984).
[4] S. V. Manson, *Correlations of Heat Transfer Data and of Friction Data for Interrupt Plain Fins Staggered in Successive Rows*, NACA Tech. Note 2237, NACA, Washington (1950).
[5] A. R. Wieting, Empirical correlation for heat transfer and flow friction characteristics of rectangular offset-fin plate-fin heat exchangers, *Journal of Heat Transfer*, 97 (1975) 488-490.
[6] H. M. Joshi and R. L. Webb, Heat transfer and friction in the

offset strip fin heat exchanger, *International Journal of Heat and Mass Transfer*, 30 (1987) 69-84.
[7] S. Mochizuki and Y. Yagi, Transport phenomena in stacks of interrupt parallel-plate surface, *Experimental of Heat Transfer*, 1 (1987) 127-140.
[8] E. V. Dubrovsky and V. Y. Vasiliev, Enhancement of convective heat transfer in rectangular ducts of interrupted surfaces, *International Journal of Heat and Mass Transfer*, 31 (1988) 807-818.
[9] R. M. Manglik and A. E. Bergles, Heat transfer and pressure drop correlations for the rectangular offset strip fin compact heat exchanger, *Experimental Thermal Fluid Science*, 10 (1995) 171-180.
[10] N. C. Dejong, L. W. Zhang, A. M. Jacobi, S. Balachandar and D. K. Tafti, A complementary experimental and numerical study of the flow and heat transfer in offset strip-fin heat exchangers, *Journal of Heat Transfer*, 120 (1998) 690-698.
[11] Y. C. Chang, Sequencing of chillers by estimating chiller power consumption using artificial neural networks, *Building and Environment*, 42 (2007) 180-188.
[12] M. Hosoz and M. H. Ertunc, Artificial neural network analysis of an automobile airconditioning system, *Energy Conversion and Management*, 47 (2006) 574-587.
[13] O. Ramzi, Building shape optimization using neural network and genetic lgorithm approach, *ASHRAE Transactions*, 112 (2006) 484-491.
[14] C. G. Juan, O. D. Jose and U. Gustavo, Film cooling optimization on leading edge gas turbine blade using differential evolution, *Journal of Aerospace Engineering*, 233 (2019) 1656-1666.
[15] P. V. Arturo, S. Mirhir, K. T. Yang and M. L. Rodney, Neural network analysis of fin-tube refrigerating heat exchanger with limited experimental data, *International Journal of Heat and Mass Transfer*, 44 (2001) 763-770.
[16] D. Gerardo, S. Mirhir, K. T. Yang and M. L. Rodney, Simulation of heat exchanger performance by artificial neural networks, *HVAC&R Research*, 5 (2011) 195-208.
[17] M. H. Esfe, Designing a neural network for predicting the heat transfer and pressure drop characteristics of Ag/water nanofluids in a heat exchanger, *Applied Thermal Engineering*, 126 (2017) 559-565.
[18] S. R. Patra, R. Jehadeesan, S. Rajeswari and S. A. V. Satyamurthy, Artificial neural network model for intermediate heat exchanger of nuclear reactor, *International Journal of Computer Applications*, 1 (2010) 63-69.
[19] A. L. London and R. K. Shah, Offset rectangular plate-fin surfaces-heat transfer and flow friction characteristics, *Journal of Engineering and Power*, 90 (1968) 218-228.
[20] F. M. Walters, *Hypersonic Research Engine Project - Phase IIA, Category I Test Report on Fin Heat Transfer and Pressure Drop Testing*, Data Item No. 63.02, AiResearch Manufacturing Co., Doc. AP-69-5348 (1969).
[21] A. L. London and C. K. Ferguson, Test results of high-performance heat-exchanger surfaces used in aircraft intercoolers and their significance for gas-turbine regenerator design, *Trans. ASME*, 71 (1949) 17-26.
[22] R. H. Norris and W. A. Spofford, High-performance fins for heat transfer, *Trans. ASME*, 64 (1942) 489-496.
[23] U. T. Joyner, *Experimental Investigation of Entrance Region Heat Transfer Coefficients*, NACA ARR 3K01, NACA, Washington (1943).
[24] E. K. Kalinin, G. A. Dreitser and E. V. Dubrovsky, Compact tube and plate-finned heat exchangers, *Heat Transfer Engineering*, 6 (1985) 44-51.

Sangmin Kim received his undergraduate degree from Pusan National University, South Korea in 2018. Currently, he is pursuing integrated Ph.D. at Pusan National University, Korea. His research interests are focused on Heat Exchanger, finite volume method, gas turbine blade, ANN and computational fluid dynamics.

Sudhanshu Pandey received his M.S. degree from Indian Institute of Technology Madras, India in 2016, and pursuing Ph.D. from Pusan National University, Korea. His research interests are focused on natural convection, non-Newtonian fluids and computational fluid dynamics.

Man Yeong Ha received his B.S. degree from Pusan National University, Korea, in 1981, M.S. degree, in 1983, from Korea Advanced Institute of Science and Technology, Korea, and Ph.D. degree from Pennsylvania State University, USA in 1990. Dr. Ha is currently a Professor at the School of Mechanical Engineering at Pusan National University in Busan, Korea. He served as an Editor of the Journal of Mechanical Science and Technology. He is the member of Honorary Editorial Advisory Board of the International Journal of Heat and Mass Transfer. His research interests are focused on thermal management, computational fluid dynamics, and micro/nano fluidics.